A 3.4–4.6GHz In-Band Full-Duplex Front-End in CMOS Using a Bi-Directional Frequency Converter

Xiang Yi[1], Jinchen Wang[1], Cheng Wang[1,2], Kenneth E. Kolodziej[3], Ruonan Han[1]

[1]Massachusetts Institute of Technology, Cambridge, MA

[2]Analog Devices, Boston, MA

[3]Massachusetts Institute of Technology, Lincoln Laboratory, Lexington, MA

The 2020 IEEE MTT-S International Microwave Symposium 23-25 June 2020 Los Angeles, CA

Outline

- Introduction
- Bi-Directional Frequency Converter: Concept
- Circuit Implementation
- Measurement Results
- Conclusion

Outline

- Introduction
- Bi-Directional Frequency Converter: Concept
- Circuit Implementation
- Measurement Results
- Conclusion

In-Band Full-Duplex (IBFD)

- Compared with half-duplex, IBFD
  - Doubles the spectral capacity
  - Simplifies transmission protocols
- Nonreciprocal circulator is critical for IBFD
  - Conventional ferrite circulator with magnetic material is bulky
  - On-chip magnetic-free circulator is promising

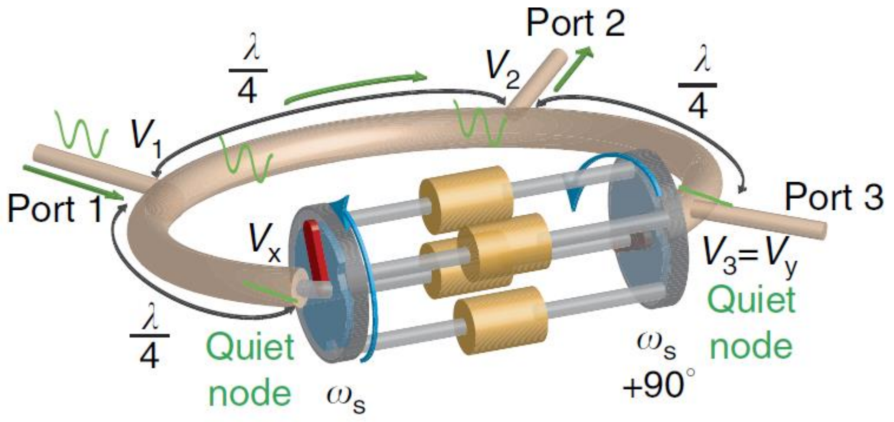

[N. Reiskarimian, *et al*., *Nat. Comm.* 2016]

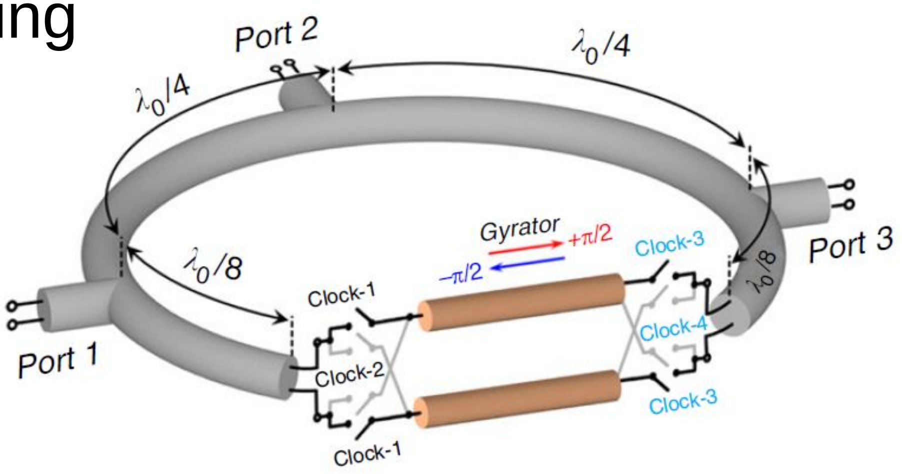

[T. Dinc, *et al*., *Nat. Comm.* 2017]

Circulator in an Integrated IBFD System

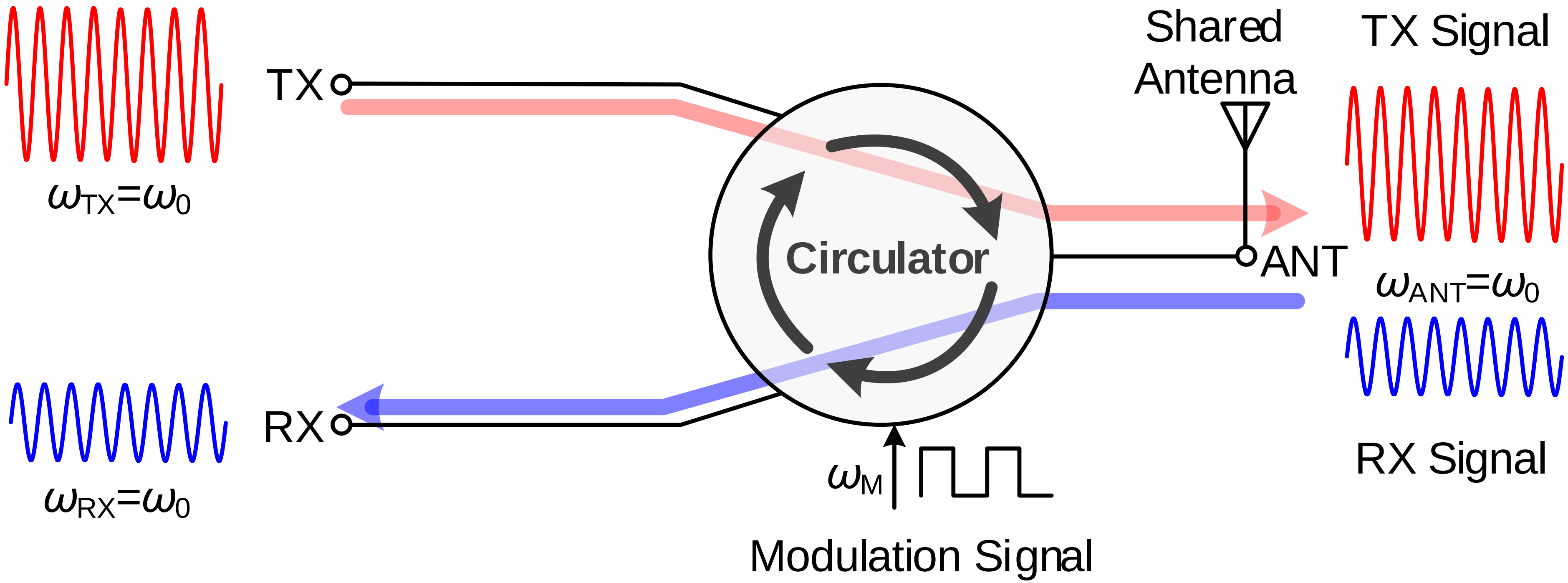

Circulator in an Integrated IBFD System

- Isolation of circulator is limited by
  - Anti-phase signal cancellation: narrow bandwidth, sensitive to mismatch

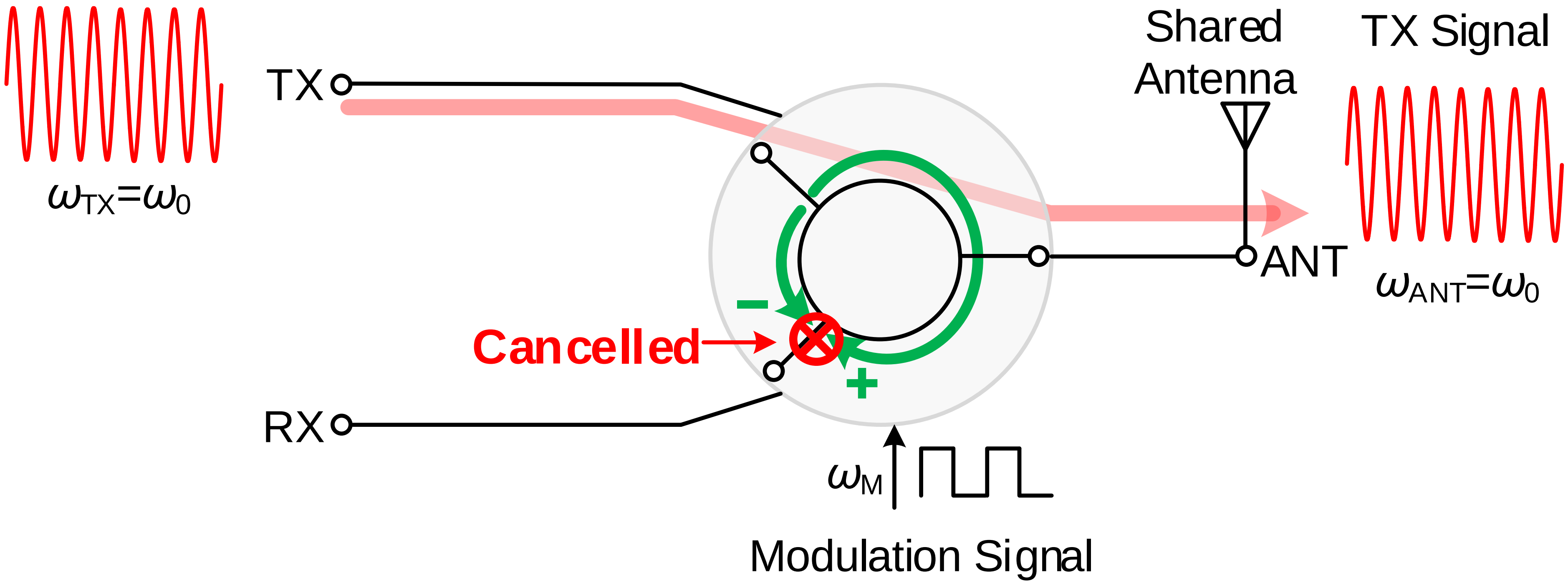

Circulator in an Integrated IBFD System

- Isolation of circulator is limited by
  - Anti-phase signal cancellation: narrow bandwidth, sensitive to mismatches
  - ANT impedance mismatch: common issue, addressed by the impedance tuner

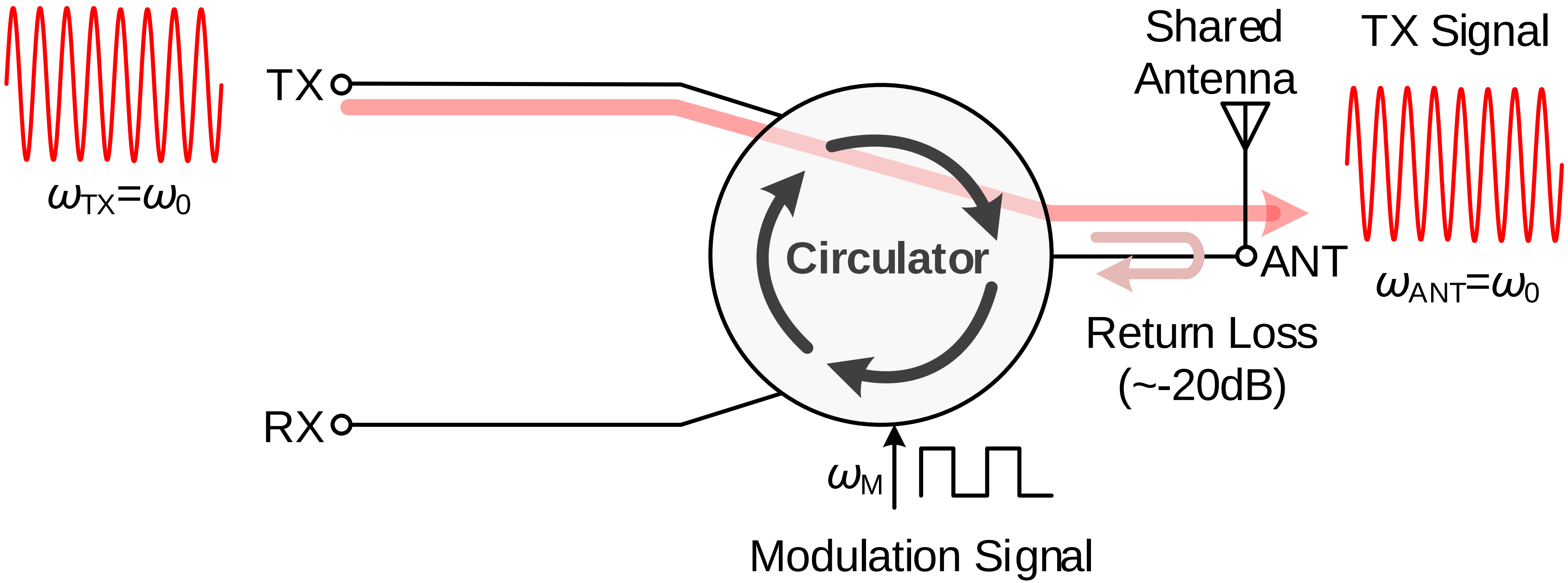

Circulator in an Integrated IBFD System

- Isolation of circulator is limited by
  - Anti-phase signal cancellation: narrow bandwidth, sensitive to mismatches
  - ANT impedance mismatch: common issue, addressed by the impedance tuner
  - On-chip coupling: silicon substrate, power lines, magnetic crosstalk

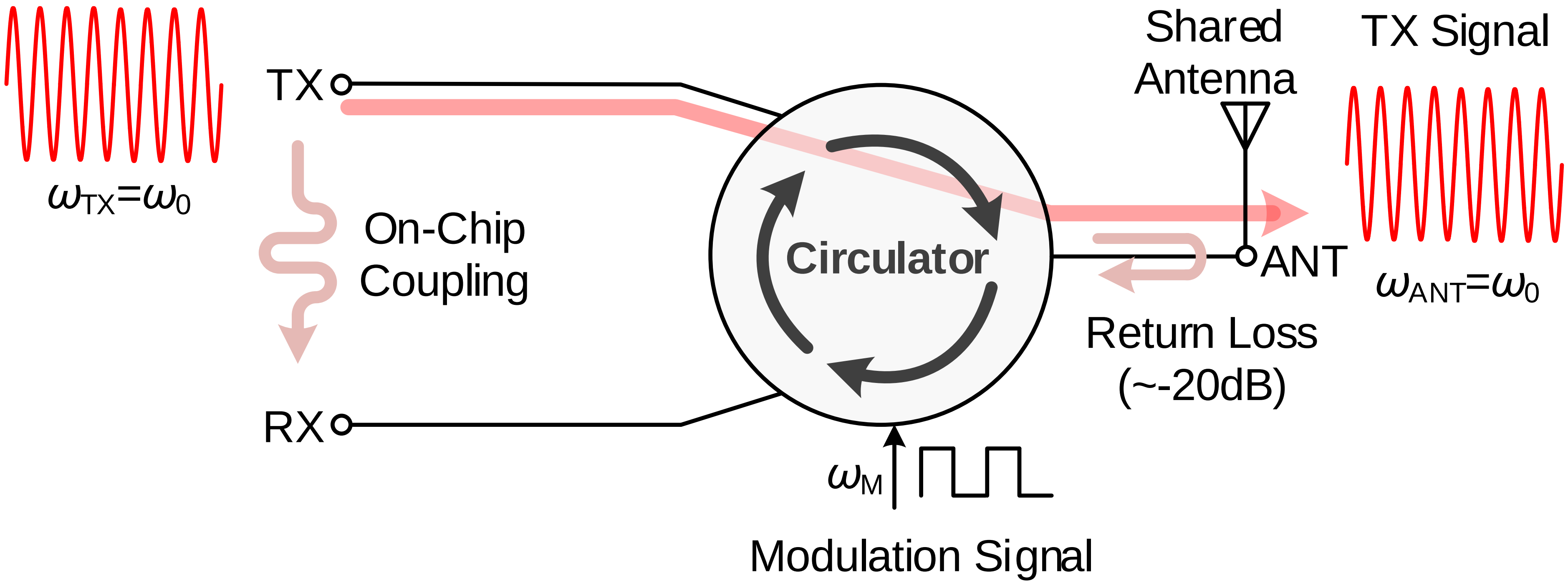

Proposed IBFD Front-End

- Bi-directional frequency converter with HPF (LPF) at TX (RX)
- Direction-independent downconversion
- $\omega_{TX} \neq \omega_{RX}$: no on-chip coupling

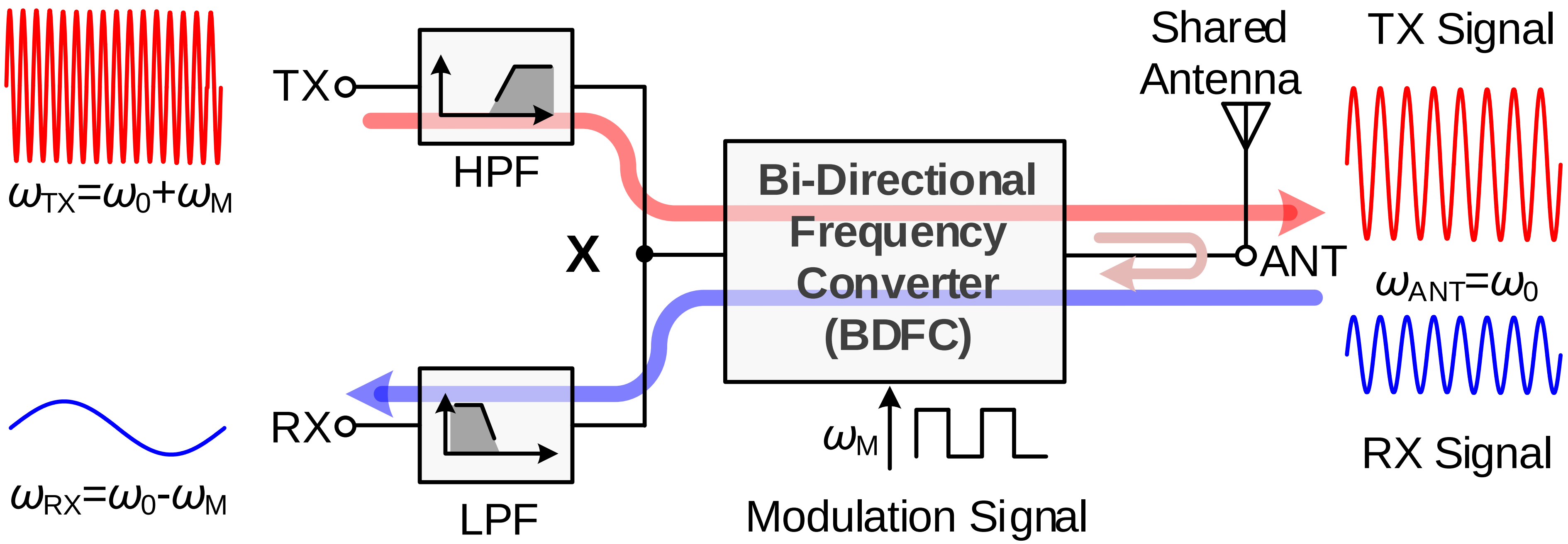

Outline

- Introduction
- Bi-Directional Frequency Converter: Concept
- Circuit Implementation
- Measurement Results
- Conclusion

Bi-Directional Frequency Converter (BDFC)

- Four parallel paths of modulated switches in series with phase shifters

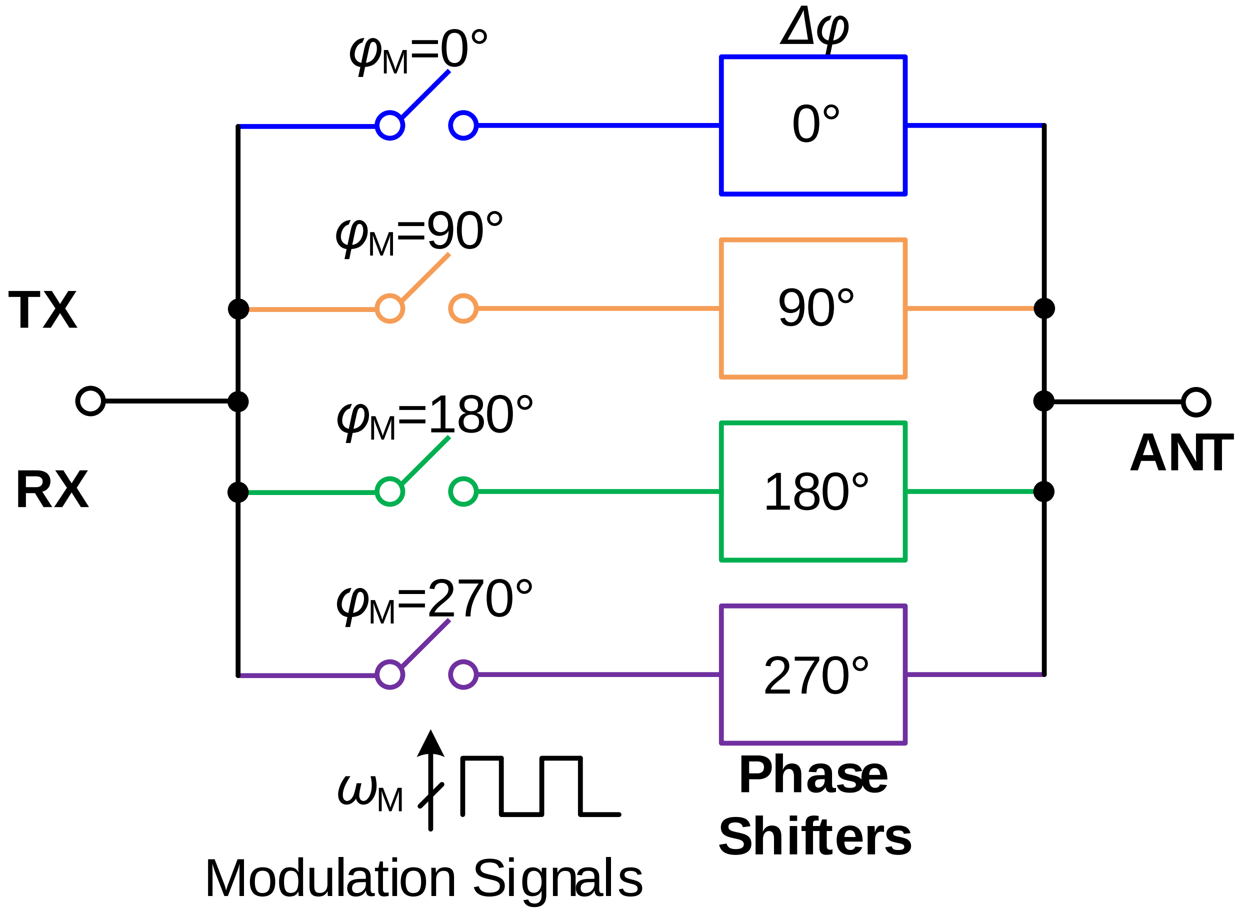

Bi-Directional Frequency Converter (BDFC)

- Four parallel paths of modulated switches in series with phase shifters
- BDFC is essentially a passive SSB mixer

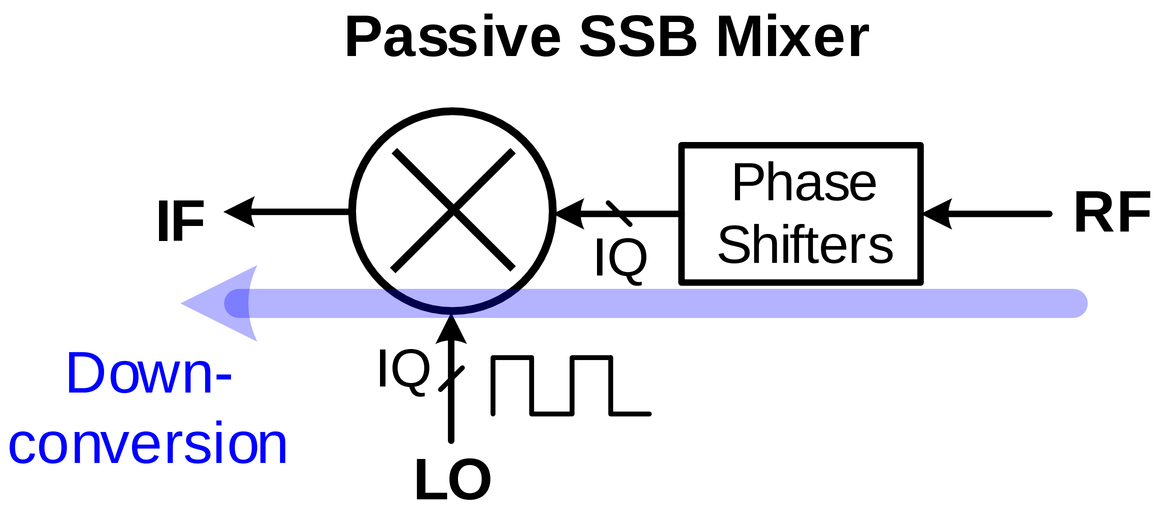

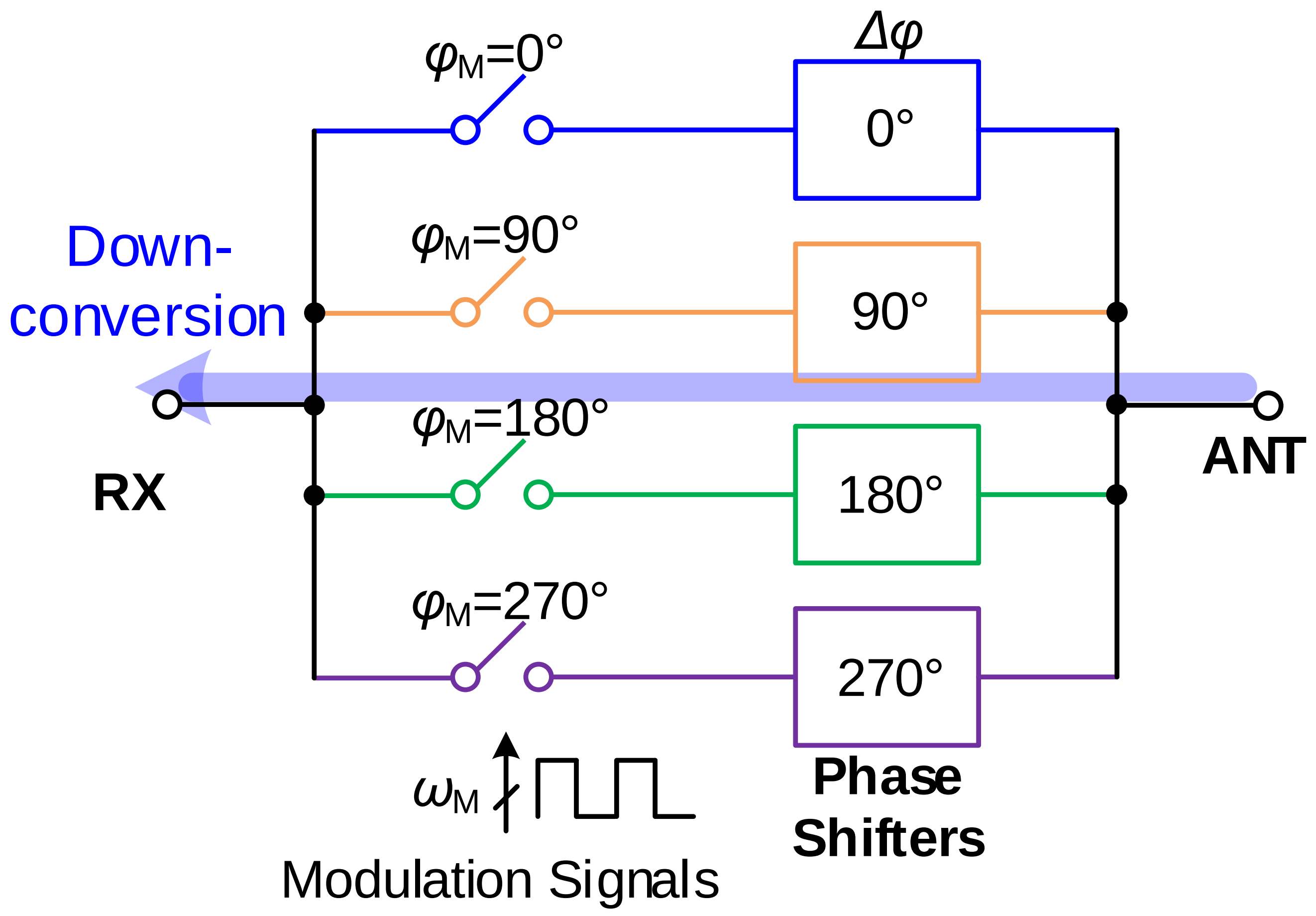

Bi-Directional Frequency Converter (BDFC)

- What happen if the signal direction reverses?
- Phasor diagram will be used to analyze the operation

Passive SSB Mixer

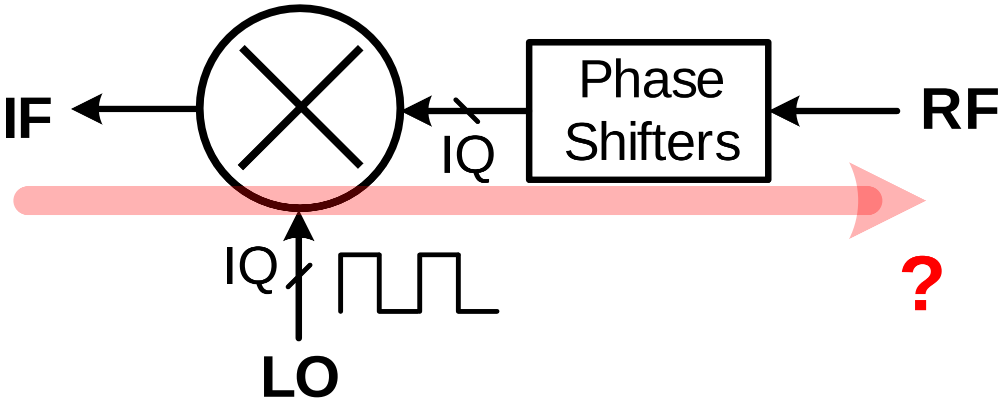

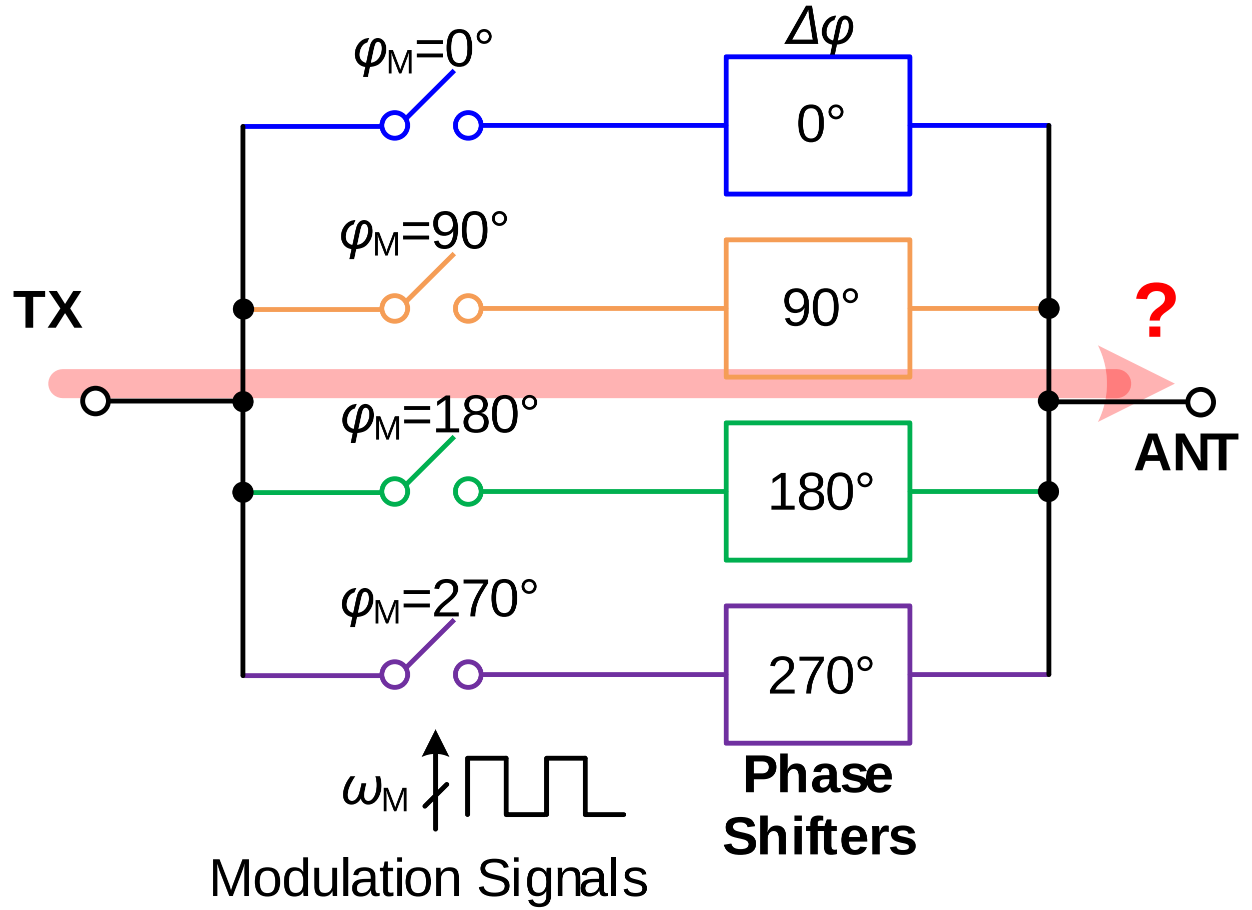

Phasors from TX to ANT

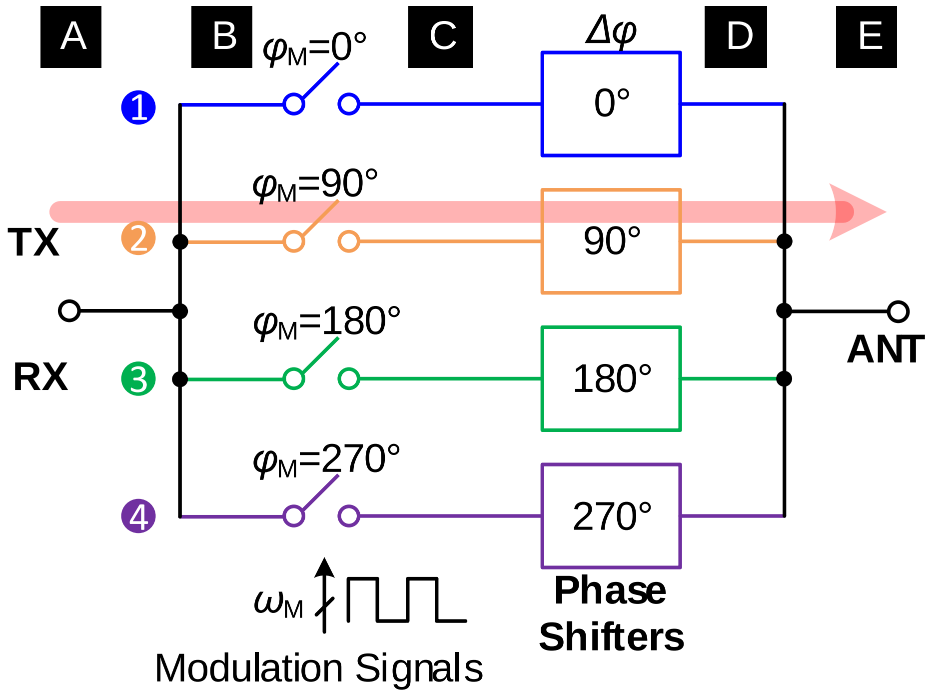

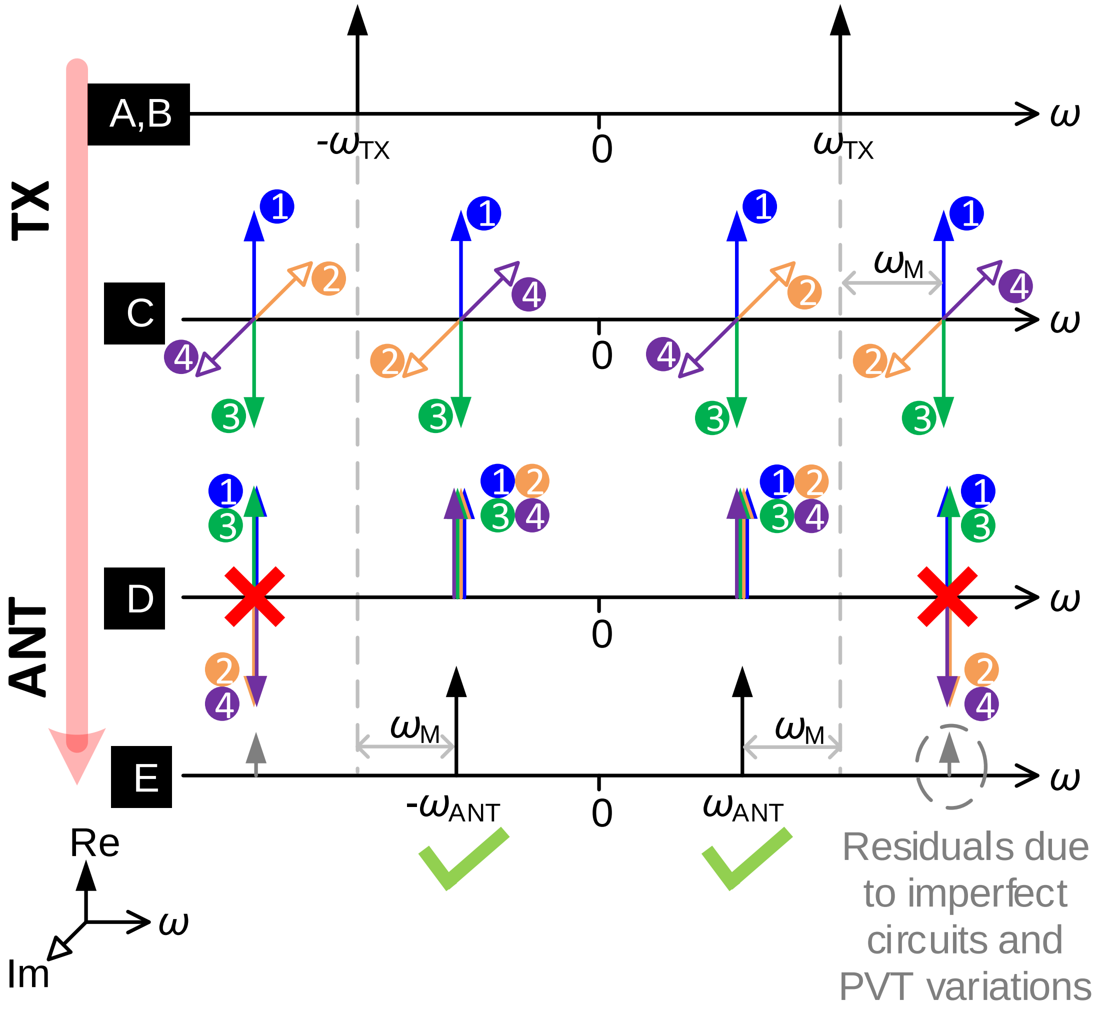

- Upper: $\sum_{i=1}^{4} exp(j((\omega_{TX} + \omega_M)t + \varphi_{M,i} + \Delta\varphi_i))$ ✗
- Lower: $\sum_{i=1}^{4} exp(j((\omega_{TX} - \omega_M)t - \varphi_{M,i} + \Delta\varphi_i))$ ✓

The switches add (subtract) frequency and phase simultaneously.

Phasors from ANT to RX

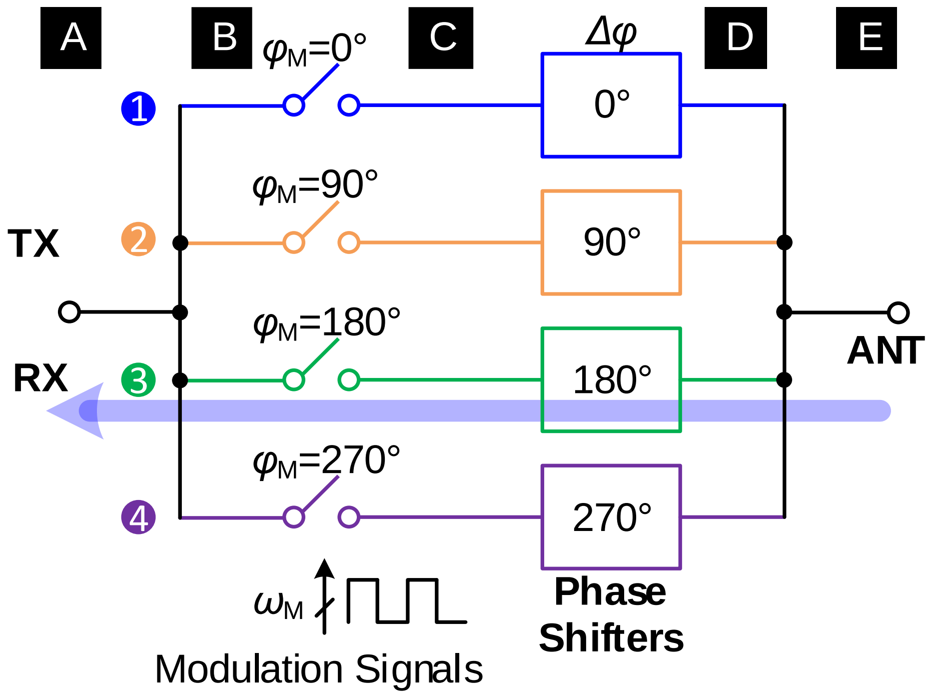

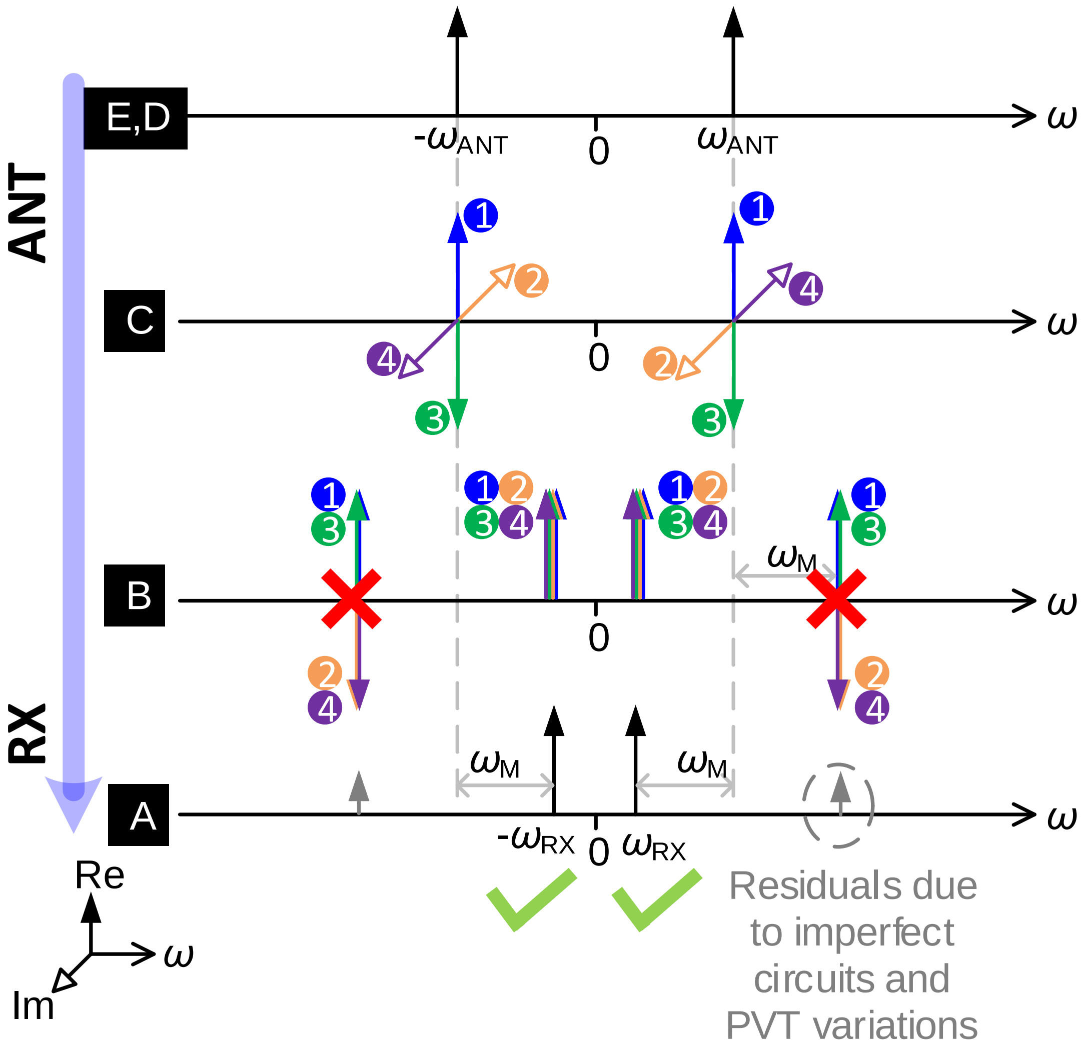

- Upper: $\sum_{i=1}^{4} exp(j((\omega_{ANT}+\omega_M)t+\varphi_{M,i}+\Delta\varphi_i))$ ✗
- Lower: $\sum_{i=1}^{4} exp(j((\omega_{ANT}-\omega_M)t-\varphi_{M,i}+\Delta\varphi_i))$ ✓

The sequence of switch and phase shifter does not matter!

Features of the BDFC-Based IBFD Front-End

- $\omega_{TX} \neq \omega_{RX}$: no on-chip coupling
- Not anti-phase signal cancellation: isolation is wideband and robust against device mismatch and non-ideal clocking
- One set of switches: high linearity
- Receiver down-mixing function
- Simple structure: compact area

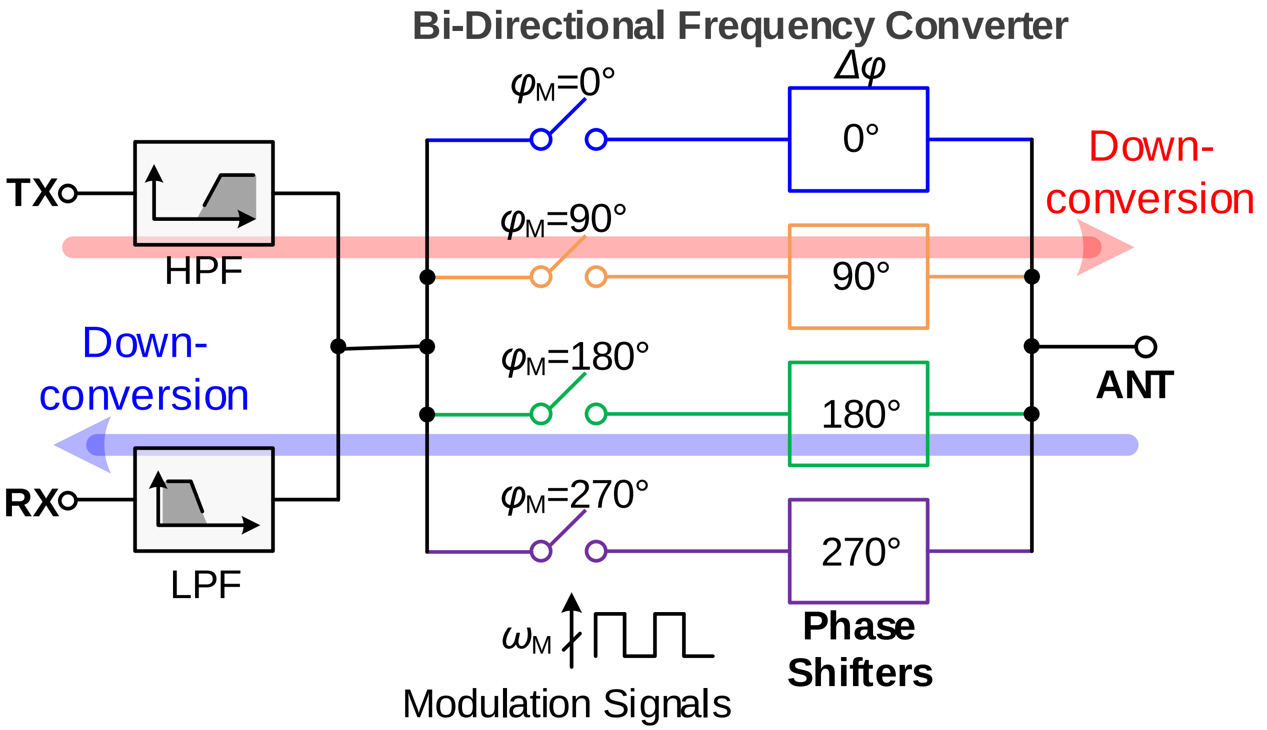

Outline

- Introduction
- Bi-Directional Frequency Converter: Concept
- Circuit Implementation
- Measurement Results
- Conclusion

Full Schematic of IBFD Front-End

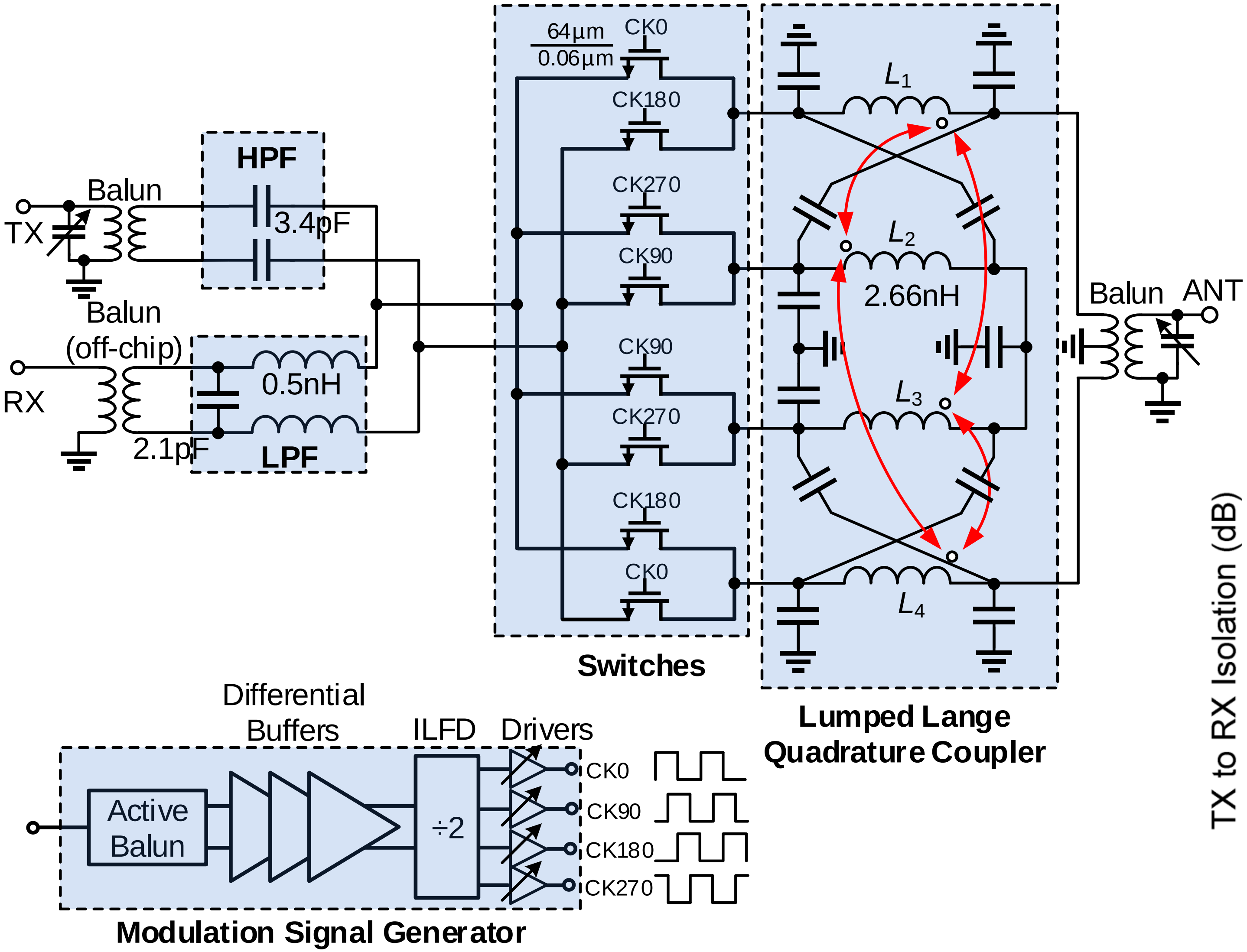

- Differential for low signal loss
- f_M =~4 GHz
- f_{TX}=~8 GHz
- f_{RX}=DC~600 MHz

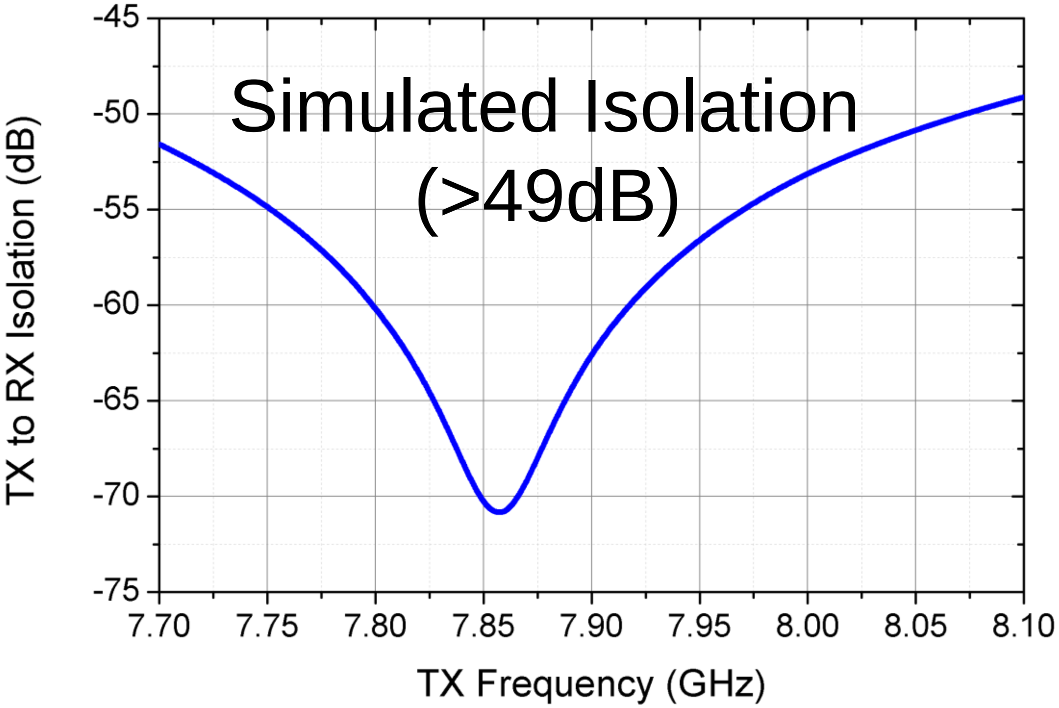

Lumped Lange Quadrature Coupler

- Four 2.5-turn inductors are coupled together: compact area
- Conversion loss: 0.7 dB at 4 GHz

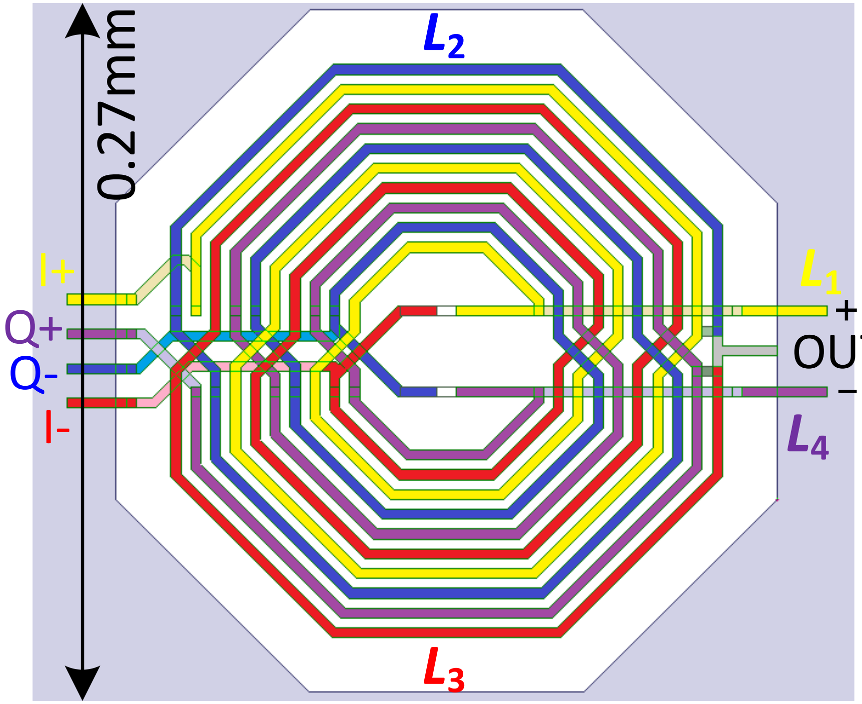

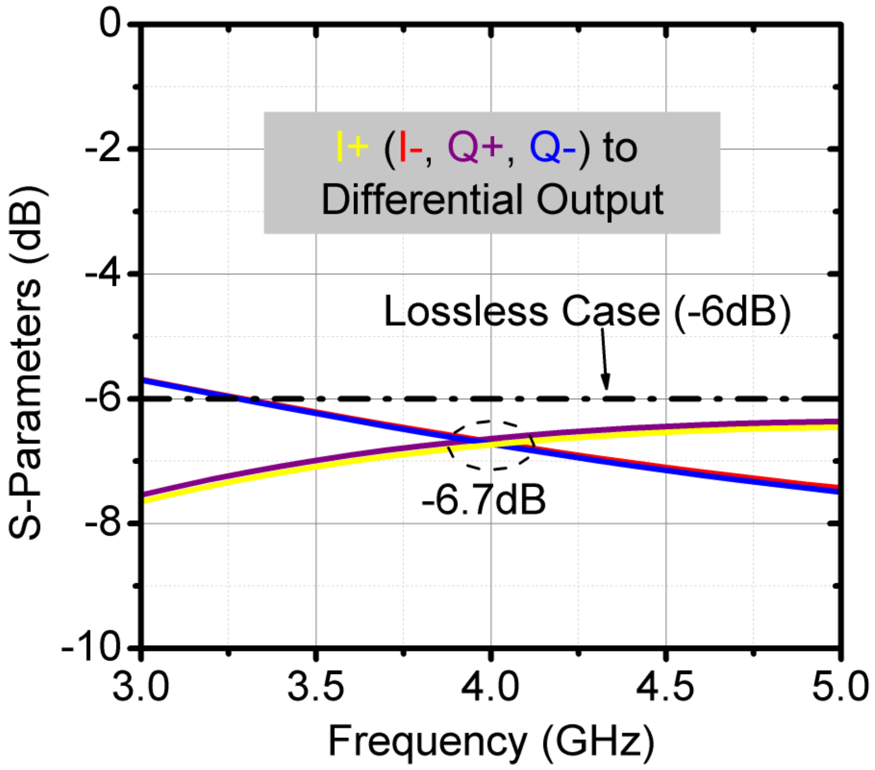

Lumped Lange Quadrature Coupler

- Four 2.5-turn inductors are coupled together: compact area
- Conversion loss: 0.7 dB at 4 GHz
- At $(\omega_{TX} + \omega_M)$, partially suppressed by band-pass characteristic

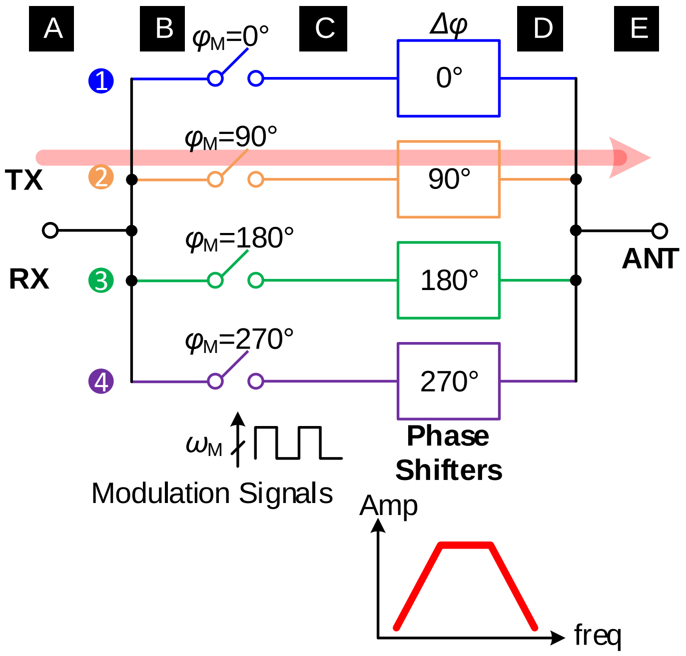

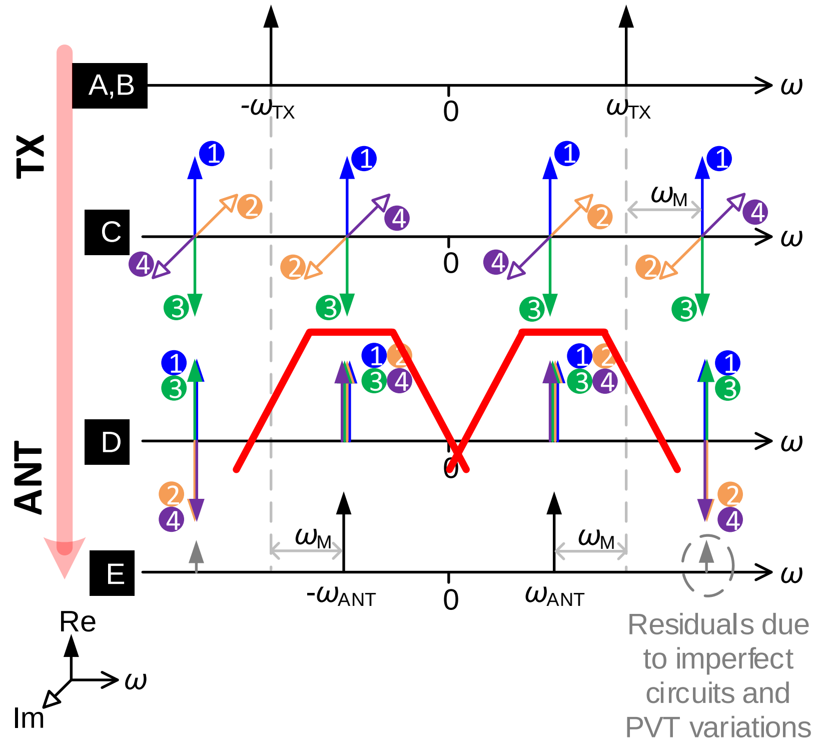

Outline

- Introduction
- Bi-Directional Frequency Converter: Concept
- Circuit Implementation
- Measurement Results
- Conclusion

Die Photo

- Low cost 65-nm bulk CMOS technology
- Compact core area: 0.72 mm by 0.37 mm

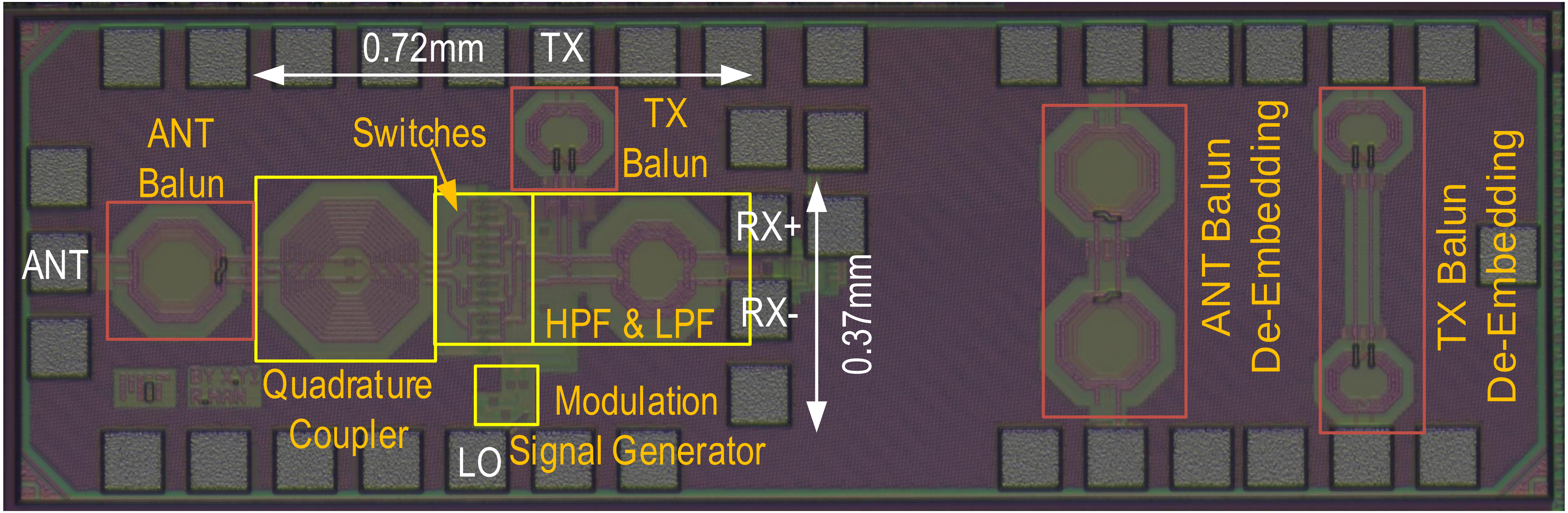

S-Parameters Measurement Setups

- ANT, TX and LO: probing
- RX balun: on PCB
- DCs and RX: wire-bonding
- Baluns' IL are de-embedded

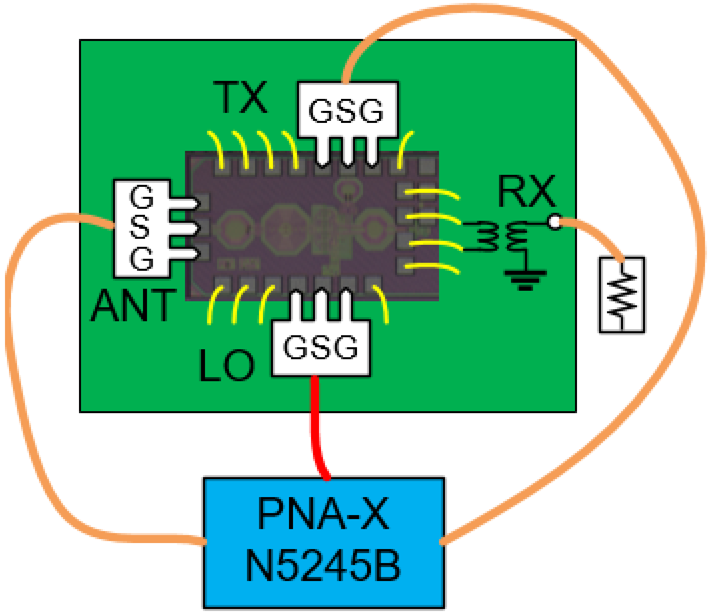

TX to ANT

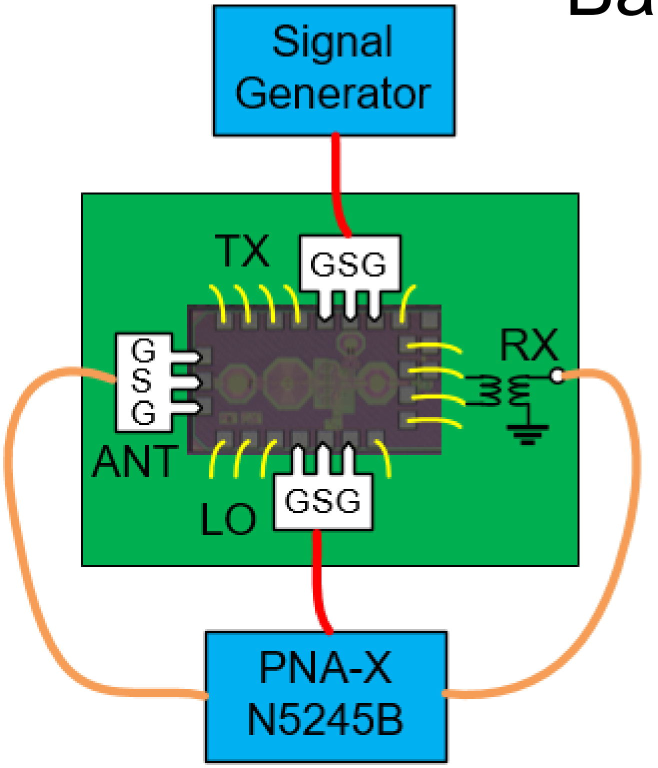

ANT to RX

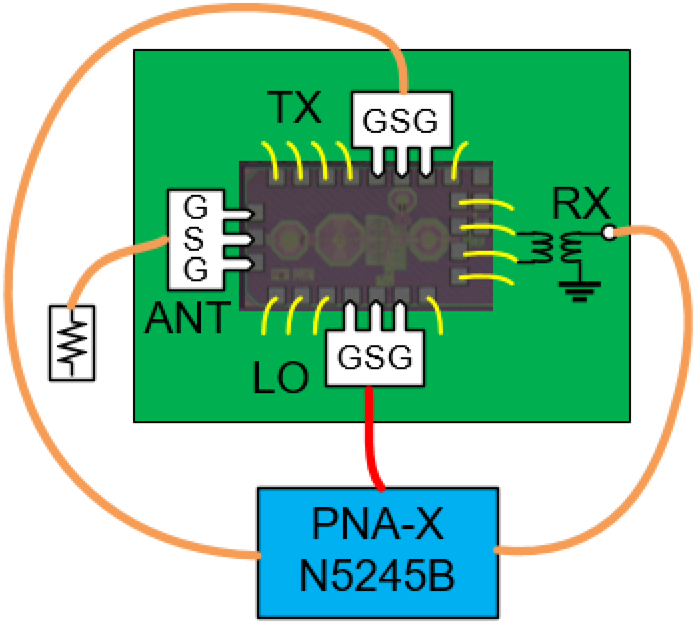

TX to RX

IBFD Front-End Measurement Results

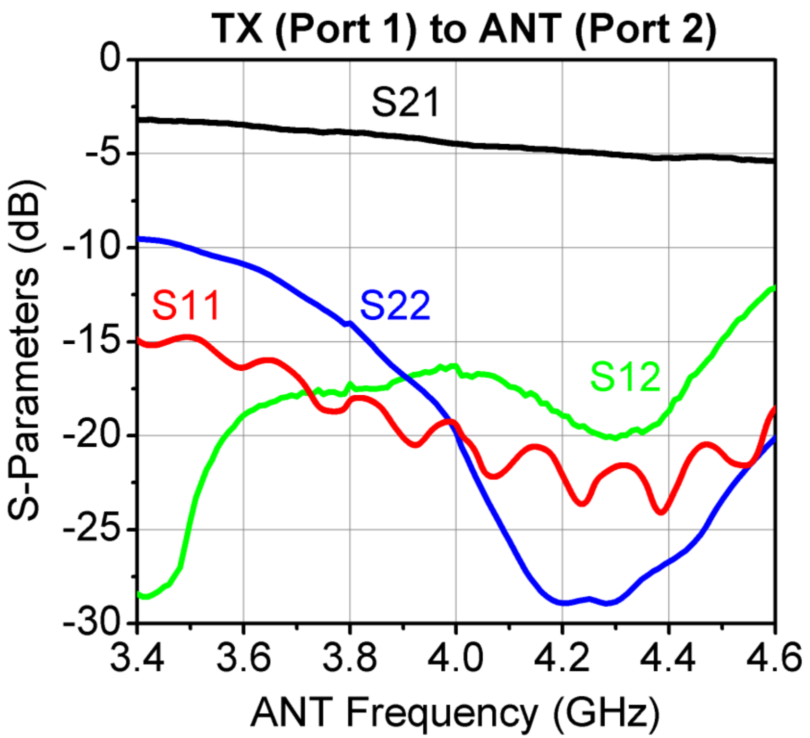

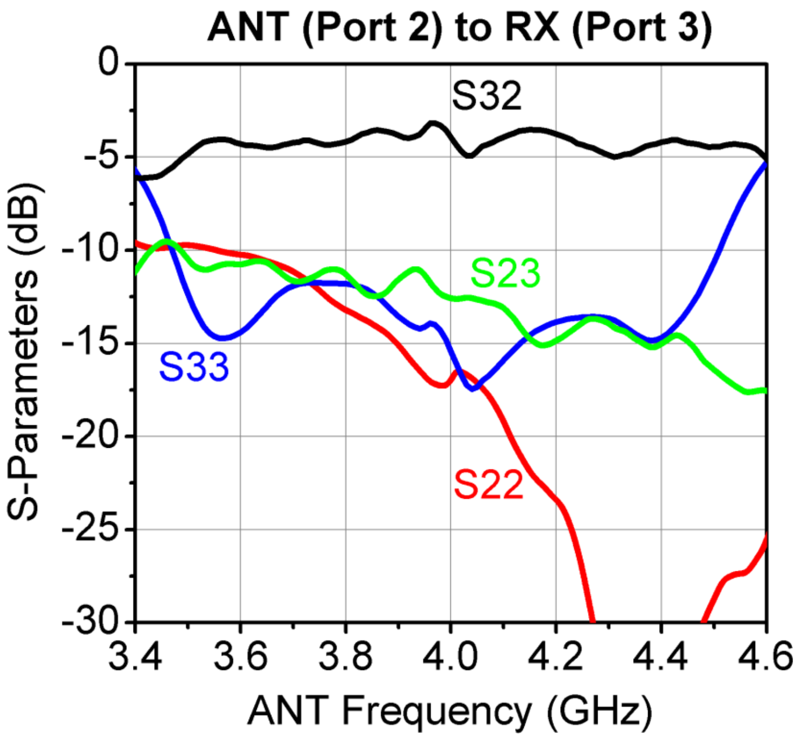

- TX-ANT Insertion Loss: 3 dB
- ANT-RX Insertion Loss: 3.2 dB

IBFD Front-End Measurement Results

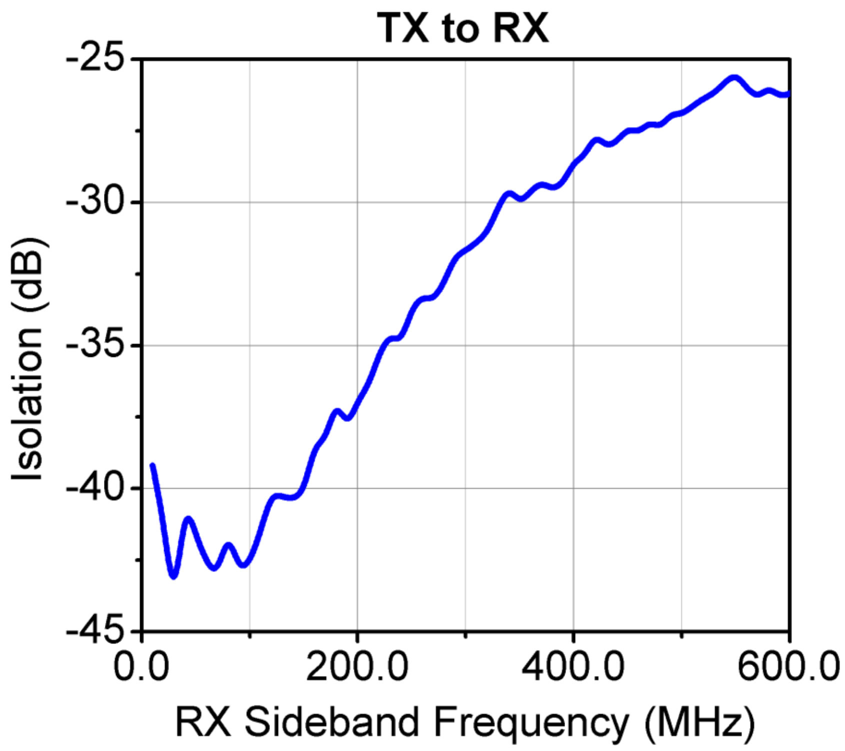

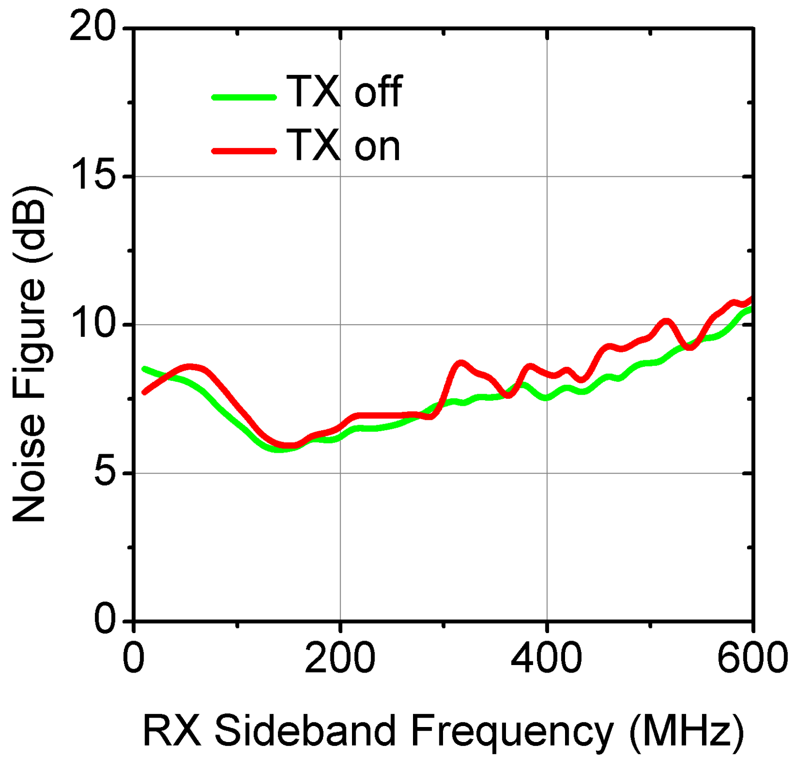

- TX-RX Isolation: 44.2~25.5 dB
- A 50 Ω load instead of an impedance tuner is used

- ANT-RX Noise Figure (TX off/on): 5.8/5.9 dB
- Receiver works in full-duplex mode

IBFD Front-End Measurement Results

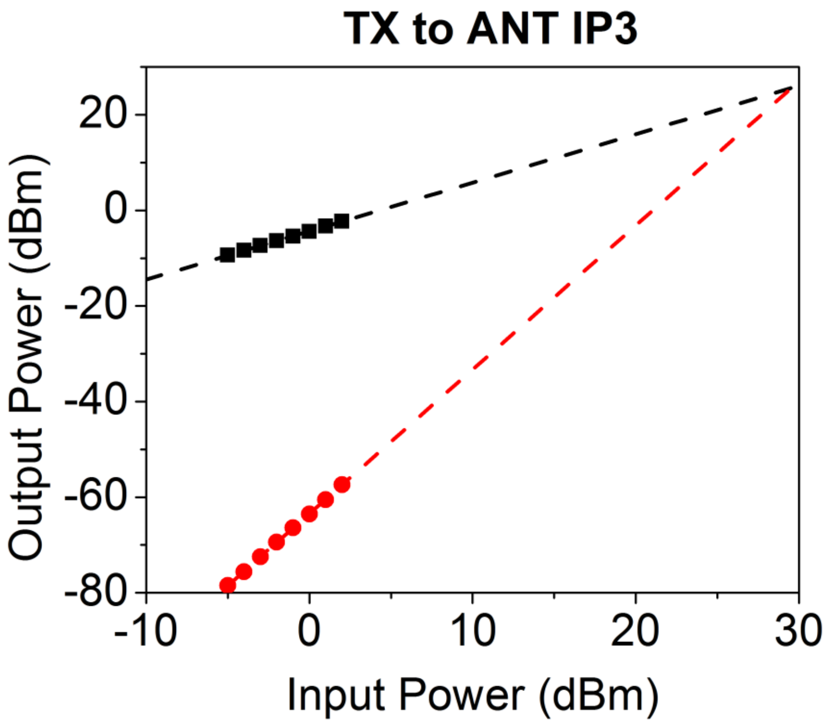

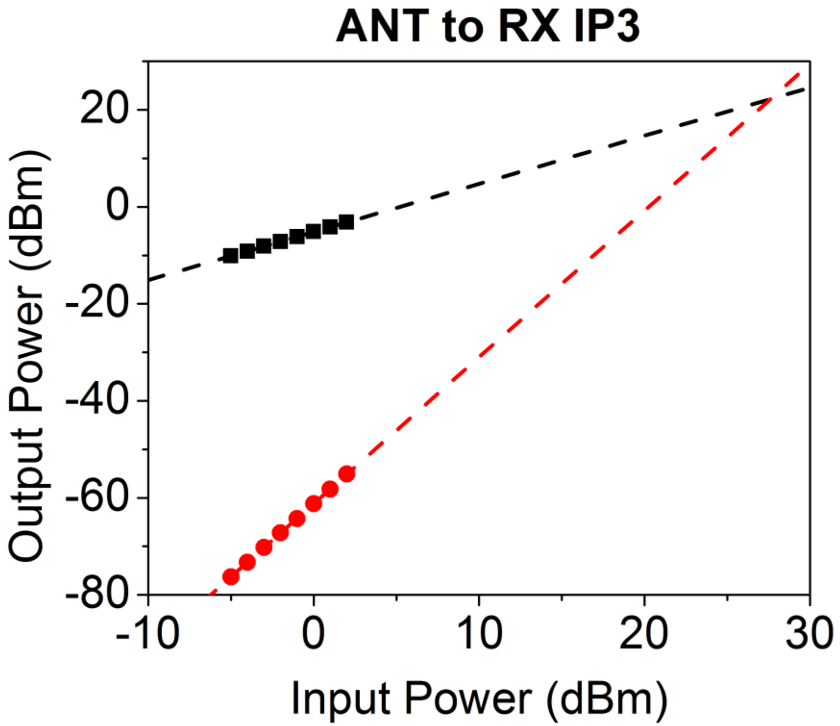

- TX-ANT IIP3: 29.5 dBm
- ANT-RX IIP3: 27.6 dBm

- Demonstrate our structure with only one set of switches in the signal path has high linearity

Comparison Table - 1

	This work	RFIC2019 [1]	JSSC2017 [2]	RFIC2018 [3]	JSSC2017 [4]	ISSCC2019 [5]
Technology	**65-nm CMOS**	40-nm CMOS	65-nm CMOS	180-nm SOI	45-nm SOI	45-nm SOI
Frequency (GHz)	**3.4~4.6**	5.6~7.4	0.65~0.85	0.86~1.08	22.7~27.3	50~56.8
Fractional Bandwidth	**30%**	28%	26.70%	17%	18%	14.60%
Isolation (dB)	**25.5**	18	15	25	18.5	20
TX-ANT/ANT-RX Insertion loss (dB)	**3.0/3.2**	2.2/2.2	1.7/1.7	2.1/2.9	3.3/3.2	3.6/3.1
Noise Figure (dB)	**5.8/5.9**[(a)]	2.4	4.3	3.2	3.3	3.2
TX-ANT/ANT-RX IIP3 (dBm)	**29.5/27.6**	17.5/17.5	27.5/8.7	50/30.7	20.1/19.9	19.4/19.0
On-Chip TX-RX Coupling	**No**	Yes	Yes	Yes	Yes	Yes
Down-Mixing for RX	**Yes**	No	Yes	No	No	No
Fully Integrated	**Yes**	Yes	No	Yes	Yes	Yes
Power Consumption (mW)	**48**	12.4	59	170	78.4	41
Core Area (mm^2)	**0.27**	0.45	25	16.5	2.16	1.72

(a) With TX off/on (0 dBm) and the homodyne RX down-conversion function included.

Comparison Table - 2

- [1] A. Ruffino, Y. Peng, F. Sebastiano, M. Babaie, and E. Charbon, “A 6.5-GHz cryogenic all-pass filter circulator in 40-nm CMOS for quantum computing applications,” in *IEEE RFIC Symposium*, 2019, pp. 107–110.
- [2] N. Reiskarimian, J. Zhou, and H. Krishnaswamy, “A CMOS passive LPTV nonmagnetic circulator and its application in a full-duplex receiver,” *IEEE J. Solid-State Circuit*, vol. 52, no. 5, pp. 1358–1372, 2017.
- [3] A. Nagulu, A. Alu, and H. Krishnaswamy, “Fully-integrated non-magnetic 180nm SOI circulator with > 1W P1dB, >+50dBm IIP3 and high isolation across 1.85 VSWR,” in *IEEE RFIC Symposium*, vol. 2018-June, 2018, pp. 104–107.
- [4] T. Dinc, A. Nagulu, and H. Krishnaswamy, “A millimeter-wave non-magnetic passive SOI CMOS circulator based on spatio-temporal conductivity modulation,” *IEEE J. Solid-State Circuits*, vol. 52, no. 12, pp. 3276–3292, 2017.
- [5] A. Nagulu and H. Krishnaswamy, “Non-magnetic 60GHz SOI CMOS circulator based on loss/dispersion-engineered switched bandpass filters,” in *Intl. Solid-State Circuits Conf.*, vol. 63, 2019, pp. 446–448.

Outline

- Introduction
- Bi-Directional Frequency Converter: Concept
- Circuit Implementation
- Measurement Results
- Conclusion

Conclusion

- A new nonreciprocity concept using frequency conversion is proposed
  - $\omega_{TX} \neq \omega_{RX}$: no on-chip coupling
  - Not anti-phase signal cancellation: isolation is wideband and robust against device mismatch and non-ideal clocking
  - One set of switches: high linearity
  - Receiver down-mixing function
  - Simple structure: compact area
- A 4-GHz CMOS prototype demonstrated our idea: wide bandwidth, high isolation, high linearity, compact area

Acknowledgments

- The authors thank Keysight for their support of testing equipment.

- This work was supported by Lincoln Laboratory (FA8702-15-D-0001).